Received January 25, 2021, accepted February 15, 2021, date of publication February 18, 2021, date of current version April 9, 2021.

Digital Object Identifier 10.1109/ACCESS.2021.3060004

Thermal Analysis of Flat Plate Solar Collector Using Different Nanofluids and Nanoparticles Percentages.

A. A. HAWWASH[1,2], MAQUSOOD AHAMED[3], S. A. NADA[1,2], ALI RADWAN[4], AND ALI K. ABDEL-RAHMAN[5]

[1]Energy Resources Engineering Department, Egypt- Japan University of Science and Technology (E-JUST), Alexandria 12577, Egypt
[2]Department of Mechanical Engineering, Benha Faculty of Engineering, Benha University, Benha 13511, Egypt
[3]King Abdullah Institute for Nanotechnology, King Saud University, Riyadh 11451, Saudi Arabia
[4]Mechanical Power Engineering Department, Mansoura University, El-Mansoura 35516, Egypt
[5]Mechanical Engineering Department, Assiut Faculty of Engineering, Assiut University, Assiut 71515, Egypt

Corresponding author: A. A. Hawwash (ahmed.hawash@ejust.edu.eg)

This work was supported by the Researchers Supporting project, King Saud University, Riyadh, Saudi Arabia, under Grant RSP-2020/129.

ABSTRACT Flat plate solar collector (FPSC) is commonly used due to its low price, less complexity, and easier installation and operation. The low thermal efficiency is the main disadvantage of this type of solar collectors. In the present study, the thermal performance of the FPSC using alumina oxide -water and copper oxide -water nanofluids are evaluated. The effect of nanoparticle volume fraction and nanoparticle type are investigated theoretically and validated experimentally. A computational fluid dynamic model is developed. The model is validated with experimental result carried in this study. The model is simulated under the hot climate conditions of Egypt. The results showed that the presence of the nanoparticles in the working fluid of the FPSC increases the pressure drop in the collector, but thermal performance enhancement is also obtained. Further, an optimum nanoparticles volume fraction of 0.5% of copper oxide nanoparticle is found to attain the highest thermal efficiency of the collector. Furthermore, using copper oxide-water nanofluid is effective than using alumina oxide-water nanofluid at the same conditions.

INDEX TERMS Flat plate solar collector, alumina and copper oxide nanoparticles, thermal model, thermal efficiency.

NOMENCLATURES

Symbol	Symbol description
A_c	The surface area of the solar collector (m2)
$(C_p)_{bf}$	The specific heat of base fluid (J/(kg K))
$(C_p)_{nf}$	The specific heat of nanofluid (J/(kg K)
$(C_p)_{np}$	The specific heat of nanoparticles (J/(kg K)
F_R	Heat removal facto
G_t	Global solar radiation (W/^{m2}
h_{back}	The convection heat transfer coefficient at the back of the collecto
K	Thermal conductivity (W/(m.K))
L	length of the tube (m)
Q_u	Rate of useful energy gained (W)
$\dot{Q}_{in}$	The heat transfer rate into the system (W)
Ra	Rayleigh number
t	Time (s)
T_a	Air temperature (K)
T_c	Glass cover temperature (K)
T_i	Inlet fluid temperature to the solar collector (K)
T_o	Outlet fluid temperature from the solar collector (K)
T_s	Sky temperature (K)
$\dot{m}$	The mass flow rate of fluid flow (kg/s)
Nu	Nusselt number
P	fluid pressure (Pa)
P_r	Prandtl number
$\dot{Q}_{out}$	The heat transfer rate out of the system (W)
u, v, w	Velocity components in x,y, z directions (m/s).
U_l	Overall loss coefficient of the solar collector (W/(m^2 K))
V_w	The wind speed (m/s)

The associate editor coordinating the review of this manuscript and approving it for publication was Dwarkadas Pralhaddas Kothari.

Greek symbols

α	Absorptivity
ρ	Reflectivity for glass and absorber, and fluid density (kg/m^3)
τ	Transmissivity
σ	Stefan-Boltzmann constant (W/(m^{2}K^4))
ϕ	The volume fraction of nanoparticles
$\tau\alpha$	Absorbance- transmittance product
μ	The viscosity of the fluid (pa.s)
β	declination angle
ε_p	Absorber plate emittance
ε_g	Glass cover emittance
η_i	Instantaneous collector efficiency

Subscripts

a	Ambient
p	Absorber plate
bf	Base fluid
c	Convection
f	Fluid
g	Glass cover
nf	nanofluid
p	Nanoparticles
r	Radiation
S	Sky
w	Wind
X	Direction of x-axis
Y	Direction of y-axis
z	Direction of z-axis

Abbreviations

ASHRAE	American Society of Heating, Refrigerating, and Air-Conditioning Engineers
DDW	Double distilled water
FPSC	Flat plate solar collector

I. INTRODUCTION

Conventional energy sources and electricity became an increasingly scarce resource all over the world. All countries are forced to consider renewable energy systems to meet their increasing demands. Solar energy can be considered the most important renewable energy source due to its sustainability, friendly environment and vital availability. Therefore the utilization of solar energy to meet the increasing demands of energy is becoming more urgent. The water heating sector, industrial applications and water desalination systems consume a considerable amount of energy. Using solar energy for water heating can save this amount of energy utilized in these applications [1]–[3]. Flat plate solar collector (FPSC), heat pipes collectors, evacuated tube collectors and concentrated solar collectors are available in the market. FPSC is considered the cheapest and simplest one for manufacturing, installation and operation [4].

Moreover, the FPSCutilizes direct and diffuse solar radiations in water heating, and it requires little cleaning and maintenance. FPSC is simply fixed at a certain tilt angle and does not need a sun tracking system. For these reasons, a flat plate collector is considered the most common collector for domestic water heating systems in many countries. The main disadvantage of the FPSC is its low thermal efficiency due to the high rate of heat losses by radiation and convection from its surface. Several types of research are devoted to enhancing the thermal performance of the FPSC [5].

For the recent two decades, nanofluids have been studied and examined extensively after the study obtained in 1995 by Choi and Eastman, which presented nanofluids [6]. While Maxwell was the first one who presented a theoretical basis to predict the effective conductivity of suspension. Nanofluid is related to a suspension mixture between liquid and tiny particles metallic or nonmetallic solids. Nanofluids are classified as a new class of fluids created by dispersing nano-sized particles in heat transfer fluid. The thermophysical properties of nanofluid could predict, theoretically [7]. On the one hand, the thermal conductivity of nanoparticles is high compared with the base fluid used in heat transfer applications, result in enhancing the heat exchange. On the other hand, the high density of nanoparticles lead to growth in the viscosity of nanofluids and increase the pressure drop and required power for pumping in forced conventional heat transfer systems [8]. The physical nanofluid properties have quite various from the base fluid. Thermal conductivity, specific heat, density and viscosity are changed. The density of solids is higher than that of liquids, in consequence, it is predicted that the nanofluid density will increase.

Said *et al.* [4] have carried out an experiment for examining the impact of TiO_2-water nanofluid as a working fluid on improving the performance of FPSC. The mass flow rates of the nanofluid diverged from 0.5 to 1.5 kg/min, while the volume fraction of the nanoparticles was 0.1% and 0.3%. Thermo-physical properties and sedimentation reduction for TiO_2 nanofluid were achieved by adding Polyethylene Glycol (PEG 400) as a dispersant. The findings showed that the energy efficiency rise to 76.6% and the highest value of exergy efficiency obtained was 16.9% for the condition of 0.1% volume fraction and 0.5 kg/min flow rate. They have shown for 0.1% and 0.3% volume fraction of TiO_2 nanofluid, the pumping power and pressure drop was equal to the base fluid. For more than one month aqueous based TiO_2 nanofluid remained stable, the thermal conductivity is influenced apparently by the volume fraction as it enhances by 6% with 0.3 vol% of TiO_2. The solar collector in case of using the TiO_2-H_2O nanofluid has higher exergy and energy efficiencies than a case of pure water.

Using nanofluids as the working fluid of the FPSC is one of the techniques used to enhance the thermal characteristics and performance of the FPSC [9], [10]. Improving the thermal performance of the FPSC by improving the thermal characteristics of the working fluid of the FPSC using nanofluids were investigated by many researchers in the last decades [7].

Dispersing nanoparticles of a high conductive material in a base fluid enhances the thermal conductivity of the fluid. The nanoparticles' high thermal conductivity and surface areas enhance the heat conduction and convection in the nanofluids [11], [12].

Choi and Stephen [6] introduced the concept of increasing the nanofluids' thermal conductivity by adding nanoparticles. They reported that adding 1% by volume concentration of the nanoparticle can double the fluid's thermal conductivity. Other researchers confirmed the results of Choi and Stephen [13]–[15]. They reported that adding a small amount of solids nanoparticles to a base fluid causes a considerable enhancement of its thermal conductivity. Nanofluids have fascinated a large interest in the last decades, because of their significant enhancement in suspension thermal properties. Keblinski *et al.* [16] showed that by adding carbon nanotubes or Cu nanoparticles in oil or ethylene glycol that have a volume of fraction lower than 1 %, the thermal conductivity of nanofluids enhanced by 150% and 40%, respectively.

Hwang *et al.* [17] measured the convective heat transfer coefficient and pressure drop of aluminium oxide nanofluid, which flows through a circular tube. They concluded that alumina nanofluids' thermal conductivity increased by about 44% due to the Alumina nanoparticles' insertion. Terekhov *et al.* [18] studied the effect of the Alumina nanoparticles percentage on improving the nanofluid's thermal conductivity of the particle size of 43nm, experimentally. They concluded that the thermal conductivity enhancement increases by about 10% maximum enhancement at a 3% volume percentage of alumina. Maïga *et al.* [19] investigated the nanofluid's thermal characteristics for both laminar and turbulent regimes in a uniformly heated tube using the single-phase model numerically. They stated the increase in Reynolds number and heat transfer coefficient with the insertion of the nanoparticles. Chandrasekar *et al.* [18] have studied experimentally the improvement in Alumina nanofluids thermal conductivity, with different volume fraction: 0.33%, 0.75%, 1%, 2% and 3%, and a particle size of 43nm. They reported that the thermal conductivity rose as the volume concentration increased with a maximum enhancement of 9.7% at 3% volume fraction.

The main problem of using the nanofluid is the stability of the nanoparticles in the fluid. Therefore, physical and chemical treatments of the nanoparticle's dispersion in the fluid are necessary to get stable nanofluids. Several preparation techniques of the nanofluid have been developed [20].

Youesfi *et al.* [21] experimentally studied the effects of inserting Alumina nanoparticles on the efficiency of FPSC for a different mass flow rate of the base fluid. They found that the collector efficiency increases by 28% if the nanoparticles of alumina is inserted into the working fluid by 0.2% weight fraction. Tyagi *et al.* [22] studied theoretically the characteristics of the FPSC using Alumina water-based nanofluid as the working fluid. It was reported that (i) the absorbed incident radiation increased nine times in the case of Alumina nanofluids comparing with pure water, and (ii) the efficiency of the FPSC in the case of using nanofluid is greater than that of pure water by 10%.

Recently, Hawash *et al.* [23], [24] presented an experimental study of the performance of the FPSC using Alumina water-based nanofluid. They examined the effect of using alumina nanofluid on the thermal performance of forced type FPSC. They showed that the efficiency of the FPSC using Alumina nanofluid with a specific percentage is higher than that of distilled water.

Lu *et al.* [25] have investigated experimentally the improvement in the evacuated tube solar collectors efficiency, via using copper oxide–water nanofluid instead of deionized water as the working medium. They showed that regarding the nanofluids as the absorption medium can significantly enhance the thermal performance of the evaporator, and there is a rise in the coefficients of evaporating heat transfer by about 30% compared with the case of deionized water. In addition, the copper oxide nanoparticles mass fraction has obvious impact on the heat transfer coefficient in the evaporation section, also the optimal mass concentration is 1.2% corresponds to an enhancement in heat transfer.

Otanicar and Golden [26] have studied the effect of using nanofluids with the aim of enhancing solar collector thermal efficiency as compared to normal solar collectors which used for domestic applications, from economic and environmental perspectives. They concluded that however, the nanofluid based solar collector has a quite longer payback period caused by the nanoparticles cost, overall after useful life it has the same economic savings like a conventional collector.

Taylor *et al.* [27] have built a model to study the graphite nanofluids impact on the efficiency of the high flux solar collector. They observed an enhancement up to 10% in the efficiency of the high flux solar collector, compared to surface-based collectors, by utilizing the nanofluids as the absorption medium.

Faizal *et al.* [28] presented theoretical investigations for pressure drop, entropy generation and heat transfer improvement inside FPSC. The absorbing medium was the suspended nanoparticles (Al_2O_3, SiO_2, CuO, TiO_2 dispersed in water), with a volume fraction range and flow rate range were (1-4) %, (1–4) l/min respectively. From Analytical perspective, the copper oxide nanofluid can decline the entropy generation by 4.34%, and increase the heat transfer coefficient by 22.15% compared to absorbing fluid water, also the pumping power decreased by 1.58%.

In another study for Otanicar *et al.* [29] who examined three kinds of nanofluids: carbon nanotubes, graphite, and silver, suspended in distilled water to be a medium on a solar collector, they examined theoretically the direct absorption solar collector based on nanofluids, and the results validated with the experimental data. They showed a remarkable initial enhancement in thermal efficiency with the volume fraction rising, but the level off as volume concentration continues to increase.

Based on the recent literature survey, although several researches were conducted to study the effect of using

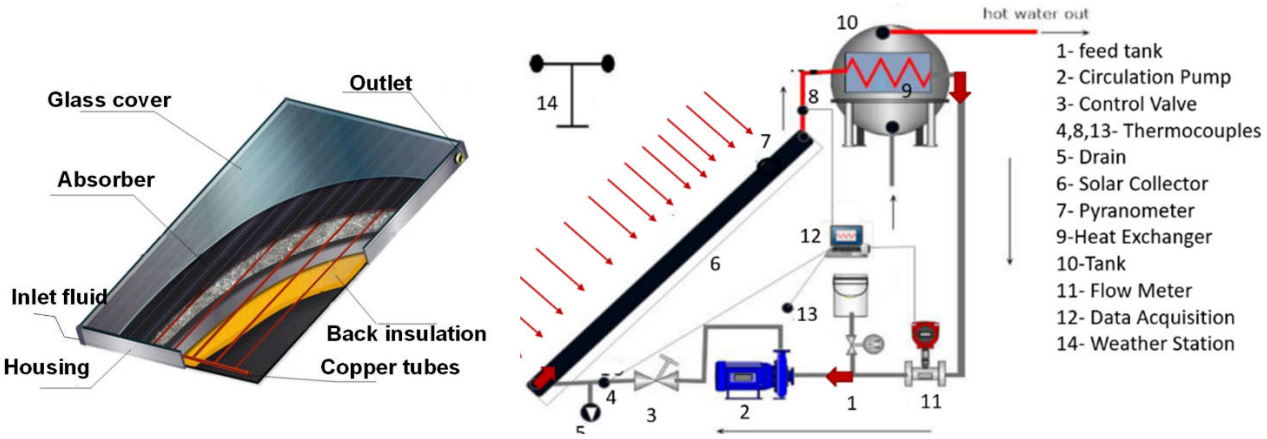

a- The solar collector layers. b- The Schematic diagram of the solar water heater.

FIGURE 1. The Layers and the Schematic diagram of the solar water heater.

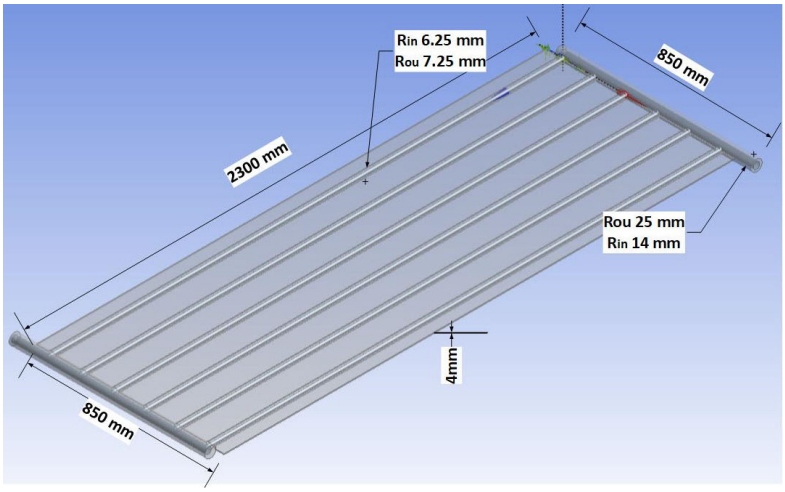

FIGURE 2. The absorber geometry of the model.

nanofluid on the thermal performance of the FPSC. Most of these researches were CFD-based researchers. Therefore, the novelty of the present study is to develop a comprehensive thermal model for the FPSC working with different nanofluids having various nanoparticle concentrations. The developed CFD model is validated with experimental work conducted in this study. In addition, this study investigates the effect of using two different two common types of nanofluids with different nanoparticle fractions. Also, the most appropriate nanoparticle volume fraction is defined.

II. PHYSICAL MODEL

Figure 1 shows a schematic diagram and layers of a commercial solar water heater. The solar collector layers are the glass cover, air gap, absorber plate, back insulation, and a working fluid. The solar water heater system consists of the solar collector, water circulation pump, storage tank with a heat exchanger, feedwater tank and control valves. The fluid passes through the piping network underneath the absorber plate. The dimensions and geometry of the absorber plate are illustrated in fig. 2. The absorber plate is made of self-coated copper. The width, length and thickness of the absorber are 850-mm, 2300-mm and 4-mm. The collector's piping system consists of two copper tube headers with an inner, outer diameter and length of 28-mm, 50-mm and 850-mm respectively.

The two headers are entirely thermal insulated. The two copper headers are connected with six riser tubes with 2300-mm length and 6.25-mm and 7.25-mm inner and outer radius. The spacing between each two riser tubes is 14.16 mm. The dimension, material types and properties of the FPSC are stated in table 1. Figure 3 shows the boundary condition used in the model.

The flow has a uniform velocity in x-direction normal to the inlet cross-section. This velocity varies depend on the mass flow rate. For nanofluid modelling, the nanofluid is assumed to be single phase. This means that changing the nanofluid type, and nanoparticle volume fractions changes the fluid properties [30]. The top half of the absorber is

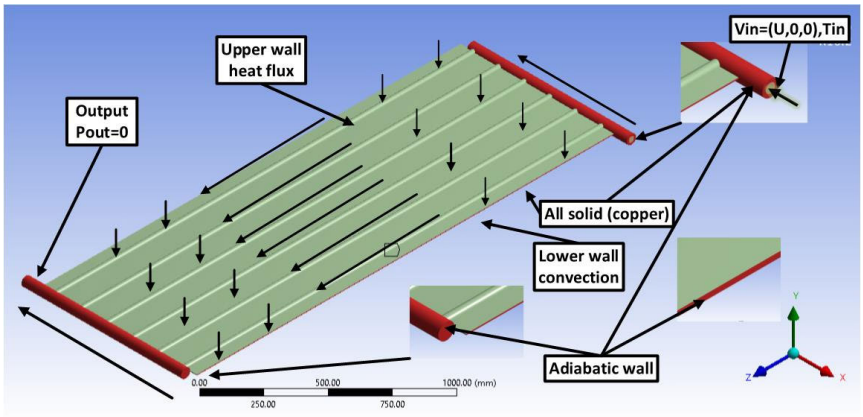

FIGURE 3. The boundary condition of the FPSC CFD model.

exposed to solar heat flux and heat loss. These values change every one hour of 8 hours, while the lower wall is exposed to a convective heat loss because of the absence of perfect insulation and it subjected to the wind. Besides, the two sides of the flat plate collector and outside surface of two headers are assumed to be adiabatic. Zero pressure gradient is employed across the outlet boundary.

In the proposed model, the following assumptions were adopted:

- The physical properties of the FPSC solid materials were considered isotropic.
- The nanofluid flow is modelled as a single phase with different properties function of nanoparticle type, base fluid properties, and nanoparticle volume fraction.
- Temperature dependent properties of water are considered in the simulation.
- The nanoparticle sedimentation during the suspension in the nanofluid is neglected. This assumption can be adopted with the use of surfactants and regular mixing of the nanofluid during the fluid flow in the FPSC.
- Perfect thermal insulation for the edges and sides of FPSC is assumed.
- The ambient temperature at the front and back of the FPSC is the same.
- Quasi-steady model is adopted.

A. EXPERIMENTAL WORK FOR VALIDATION

Hawash *et al.* [24] examined the flat plate collector experimentally with double distilled water and Alumina nanofluids. The experimental setup is stated in fig. 4. The dimension and material properties of the setup are illustrated in table 1. The working fluid of the FPSC enters the collector piping network at the bottom header and flow in the risers' pipes to absorb the solar thermal heat collected by the absorber plat and then exits the collector from the top header. For the sake of model validation with the available experimental work, the collector was examined under the hot climate condition, according to ASHRAE Standard 86-93 [1]. The location was

FIGURE 4. The setup which carried out by Hawwash *et al.* [24].

at outdoors of Energy Resources Engineering (ERE) building roof at Egypt-Japan University of Science and Technology (E-JUST) in New Borg El-Arab city, Alexandria, Egypt (Longitude/Latitude: E 029° 42' / N 30° 55'). The measured metrological data of this location are considered in the present model [24]. The solar collector is assumed to be installed with a 30° tilt angle for maximum captured radiation. They prepared alumina nanofluid using an ultrasonic vibrator (UP-200S) and disperser 500W (T18D, IKA). The solar radiation was recorded by pyranometer (WE 300)

III. MATHEMATICAL MODEL

A. GOVERNING EQUATIONS

The useful absorbed energy collected by the working fluid Q_u is [5]:

$$Q_u = \dot{m} C_p (T_o - T_i) \tag{1}$$

where C_p is the heat capacity of working fluid. The useful absorbed energy can also be calculated from the difference between the collector absorbed energy and the collector heat losses [31];

$$Q_u = F_R A_c (G_t(\tau\alpha) - U_l(T_i - T_a)) \tag{2}$$

TABLE 1. The material properties and specification of flat plate solar collector.

Absorber plate	
Dimensions (mm)	2300 x850
Absorption area (mm^2)	$1.955*10^6$
Material	Copper
Thermal Emission	7%
Solar Absorption	96%
Coating Method	Black selective coating
Sides and back Insulation	
Material	Polyurethane (40 kg/m^3)
Back thickness (mm)	40
Sides thickness (mm)	20
Covering Glass	
Thickness (mm)	3
Transmittance	91%
Absorber Piping	
Material	Copper
The diameter of headers pipe (mm)	28
No of riser pipes	6
The diameter of riser's pipes (mm)	12.5
Spacing between risers' pipes (mm)	14.16
Volume for working fluid (Liter)	4
Seal (Anti-leakage)	
Material	Rubber (E.P.D.M)

F_R, and U_lU_l are known as the collector heat removal factor and overall heat losses coefficient. Ac is the gross collector area, G_t is the solar radiation, $\tau\alpha$ is the absorbance transmittance product, and T_a is the ambient temperature. The instantaneous efficiency $\eta_i\eta_i$ is known as the ratio of energy gain to the total radiation gathered by the solar collector surface and determined from [32]:

$$\eta_i = \frac{Q_u}{A_c G_t} = \frac{m^{\cdot} C_p (T_o - T_i)}{A_c G_t} \tag{3}$$

$$\eta_i = F_R(\tau\alpha) - F_R U_l \frac{T_i - T_a}{G_t} \tag{4}$$

The fluid temperatures and pressure at the collector's outlet were calculated by applying and solving the continuity, momentum and energy equations with their boundary conditions. The weather data parameters of the location, including solar intensity, ambient air temperature and wind speed, are used as input parameters to the model. The energy conservation equation is applied to every component of the collector, including the glass cover, the absorber plate, the air gap, the collector insulation and the working fluid flow in the absorber pipe network. The continuity and momentum equations are applied to the flowing working fluid inside the absorber pipe network.

A CFD modelling was conducted to find the temperature and pressure distributions in the collector's pipe network for the different working fluid, including distilled water and different nanofluids of different concentrations. Three-dimensional steady flow mass, momentum, and energy equations for forced convection of water and nanofluid flow are given in the following equations [33].

B. MASS CONSERVATION

$$\frac{\partial(\rho u)}{\partial x} + \frac{\partial(\rho v)}{\partial y} + \frac{\partial(\rho w)}{\partial z} = 0 \tag{5}$$

where *(u, v, w)* are the velocities components at x, y and z directions (m/s).

C. MOMENTUM EQUATION

$$\rho u\frac{\partial u}{\partial x} + \rho v\frac{\partial u}{\partial y} + \rho w\frac{\partial u}{\partial z} = -\frac{\partial p}{\partial x} + \mu\left[\frac{\partial^2 u}{\partial x^2} + \frac{\partial^2 u}{\partial y^2} + \frac{\partial^2 u}{\partial z^2}\right] \tag{6}$$

$$\rho u\frac{\partial v}{\partial x} + \rho v\frac{\partial v}{\partial y} + \rho w\frac{\partial v}{\partial z} = -\frac{\partial p}{\partial y} + \mu\left[\frac{\partial^2 v}{\partial x^2} + \frac{\partial^2 v}{\partial y^2} + \frac{\partial^2 v}{\partial z^2}\right] \tag{7}$$

$$\rho u\frac{\partial w}{\partial x} + \rho v\frac{\partial w}{\partial y} + \rho w\frac{\partial w}{\partial z} = -\frac{\partial p}{\partial z} + \mu\left[\frac{\partial^2 w}{\partial x^2} + \frac{\partial^2 w}{\partial y^2} + \frac{\partial^2 w}{\partial z^2}\right] \tag{8}$$

where ρ is the fluid density, P is the fluid pressure and μ is the fluid's viscosity.

D. ENERGY BALANCE

The heat conduction equation through each layer of the collector is:

$$\frac{\partial}{\partial x}\left(k\frac{\partial T}{\partial x}\right) + \frac{\partial}{\partial y}\left(k\frac{\partial T}{\partial y}\right) + \frac{\partial}{\partial z}\left(k\frac{\partial T}{\partial z}\right) = q \tag{9}$$

where T and k are the working fluid temperature and thermal conductivity, respectively, and q is the heat absorbed due to the solar radiation per unit volume. The convection heat transfer coefficient from the glass cover (h_g), the back of the collector (h_b) and the air gap are calculated in terms

of the wind speed (V_w) and the collector characteristics as follows [5].

$$h_g = 5.28 + 4.07V_w \tag{10}$$

$$h_b = \frac{1}{2}h_g \tag{11}$$

$$h_a = \frac{Nu_a k_a}{\delta_a} \tag{12}$$

where δ_a is the air gap thickness, k_a is the air thermal conductivity and Nu_a is the air gap Nusselt number that can be calculated [34].

$$Nu_a = 1 + 1.44\left[1 - \frac{1708\left[\sin\left(1.8\beta\right)\right]^{1.6}}{Ra_j \cos\left(\beta\right)}\right]\left(1 - \frac{1708}{Ra\cos\left(\beta\right)}\right)^{+} + \left[\left(\frac{Ra\cos\left(\beta\right)}{5830}\right)^{1/3} - 1\right] \tag{13}$$

$$Ra = \frac{g\beta\Delta TL^3}{v\alpha} \tag{14}$$

R_a is the Rayleigh number, L is the tube length, β is the collector inclination angle and α is the air thermal diffusivity. The term with "+" exponent has considered only positive values; otherwise, it is set to zero. The sky temperature (T_s) can be obtained from the ambient temperature (T_a) using the following simple relation given by Culf and Gash [35], assuming the sky as a black body.

$$T_S = 0.0522.T_a^{1.5} \tag{15}$$

The heat transfer coefficient by the exchanged radiation between the absorber plate and the cover glass can be calculated from equation [5].

$$h_r = \frac{\sigma\left(T_p^2 + T_g^2\right)\left(T_p + T_g\right)}{\left(\frac{1}{\varepsilon_p}\right) + \left(\frac{1}{\varepsilon_g}\right) - 1} \tag{16}$$

where σ is Stefan-Boltzmann constant, ε is emissivity, and T_p and T_g are the average plate and glass temperatures.

E. PHYSICAL PROPERTIES OF NANOFLUIDS AND DISTILLED WATER

Calculating the thermophysical properties of the nanofluids have been suggested by different researchers [36]. It is a function of the base fluid's thermophysical properties and the nanoparticles and the percentage of the nanoparticles. The following equations give the most common correlations for the density, specific heat, viscosity and thermal conductivities [37], [38].

$$\rho_{nf} = (1 - \emptyset)\,\rho_{bf} + \emptyset\rho_p \tag{17}$$

$$(C_p)_{nf} = \frac{(1 - \emptyset)\,(\rho C_p)_{bf} + \emptyset(\rho C_p)_p}{\rho_{nf}} \tag{18}$$

$$\mu_{nf} = (1 + 2.5\emptyset + 6.5)\,\mu_f \tag{19}$$

$$K_{nf} = \left[\frac{K_p + 2K_{bf} - 2\emptyset\left(K_{bf} - K_p\right)}{K_p + 2K_{bf} + \emptyset\left(K_{bf} - K_p\right)}\right]K_{bf} \tag{20}$$

TABLE 2. The thermophysical properties of the nanoparticles; Alumina and Copper Oxide.

Nanoparticles	Alumina	Copper Oxide
Size of particles (nm)	Less than 20	
Shape of particles	Spherical	
Density (kg/m^3)	3600	6000
Thermal conductivity (W/(mK))	30	33
Specific heat coefficient (J/(kg K))	880	551

TABLE 3. Constants of Equation. 16 for the thermophysical properties of nanofluid (ρ, μ, Cp, and k).

	ρ	μ	C_p	k
A	-1.319 x10^{-7}	3.533 x10^{-11}	3.3217 x10^{-6}	6.2068 x10^{-10}
B	1.8457 x10^{-4}	-4.814 x10^{-8}	-4.4598 x10^{-3}	-8.0897 x10^{-7}
C	-9.943 x10^{-2}	2.464 x10^{-5}	2.2487 x10^{2}	-3.8437 x10^{-4}
D	23.280	-0.00561	-5.0415 x10^{2}	-7.757 x10^{-2}
E	1113.5	0.4828	46.545	6.102

where nf, bf, p and Φ refer to the nanofluid properties, base fluid and nanoparticle and the particle volume fraction, respectively. The nanoparticles' thermophysical properties in this study are given in Table2.

The dependence of the working fluid's thermophysical properties on the temperature and the nanoparticles' concentration is considered in the model. The density, viscosity, heat capacity and thermal conductivity (ρ, μ, C_p, k) of the double-distilled water and nanofluids are given in terms of the temperature by the following fourth-order polynomial equation exist in [39]:

$$\rho, \mu, C_p \text{ or } k = AT^4 + BT^3 - CT^2 + DT + E \tag{21}$$

where the constants A, B, C, D and E for ρ, μ, C_p, and k estimations are stated in Table 3, respectively.

The nanofluid properties are considered as a function of water and nanoparticles thermophysical properties, nanoparticle type, and the nanoparticle volume fractions [39]. In addition, water properties are considered as temperature dependant. Other correlations for the nanofluids thermophysical properties in terms of temperature are available in the literature. However, these empirical correlations may have better accuracy; their validity is limited for specific temperature range and concentrations. Moreover, it was reported that

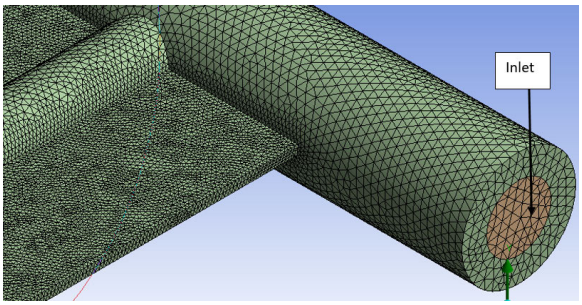

FIGURE 5. Mesh generated at the inlet side of the header.

the deviation between the predictions of the theoretical and experimental correlations for the thermophysical properties is minimal and can be neglected [40].

F. MESH GENERATION

Grid-independence test is a vital parameter to compromise between the computational accuracy and the calculation time. As increasing the number of elements increase the accuracy but requires more calculation time. However, in the current model, the total number of generated elements are about 50 million cells using academic research license of ANSYS. These number of elements are very lager enough to obtain accurate results regardless of the computational time. The mesh details were depicted in table 4 and fig. 5. After conducting the simulation, the results were found to be in a good agreement with the experiment as seen in Fig. 6.

Coarse meshes are used in an area where no physical phenomenon is expected to occur. Finer meshes are used in the transition areas like the area of connection of the header tubes with the riser pipes and the entry and exit regions of the working fluid. Figure 5 states the mesh distribution of the absorber, riser tube and header tube. Due to the collector's broad area and the high numbers of connections between the header and riser tubes, the mesh generation process is very complicated. The expected number of meshes is very high and needs a high-performance computer. Table 4 shows the properties of the mesh used in the model.

G. SOLUTION PROCEDURE

The method and procedure of the solution of the presented model can be summarized in the following steps:

- The input parameters, such as the radiation intensity, ambient temperature, wind speed, and mass flow rate of the working fluid, are assigned as per the collector location and tested flow rates.
- Initial values of the absorber temperature and glass cover are initially assumed.
- Use the model equations to calculate the sky temperature, convection, and radiation heat transfer coefficients for the collector's different parts.
- The updated values of the absorber and glass temperatures and the heat flux absorbed by the absorber plate and gained by the working fluid are found.

TABLE 4. The properties of a mesh generated inside the model.

Sizing	
Maximum size	129.04 mm
Minimum size	0.6452 mm
Smoothing	Medium
Span angel center	Fine
Statistics	
Nodes number	22,320,104
Elements number	49,167,564
Inflation	
Automatic inflation	yes
Option	Smooth
Max layers	5
Growth rate	1.2
Transition ratio	0.272

- The continuity, momentum and energy equations are numerically solved to find the working fluid temperature distribution, the pressure drop and the flow characteristics inside the absorber plate's pipe network.
- ANSYS model is used to update the thermophysical properties of the nanofluids continually.
- ANSYS model is used to estimate the thermal performance and characteristics of the FPSC.

H. MODEL VALIDATION

To validate the present model, the integrated CFD model was simulated under the same input and geometric parameter of the experimental work for DDW and Alumina nanofluids of 0.15% volume fraction. The obtained results are compared with the experimental results of Hawash *et al.* [24].

Figure 6 shows the comparison between the model prediction of the collector fluid outlet temperature and the one measured by Hawash [24] for water and alumina-water nanofluids in two different days. As shown in the figure, fair agreements between the present model predictions and the experimental data of Hawash [24] were obtained with maximum deviations of 10 % and 29 % in the case of water and alumina nanofluids, respectively. The deviation of the alumina nanofluids compared to the DDW can be attributed to the error in the model prediction for the nanofluid's thermophysical properties and the dispersion of the nanofluid that was noticed in the experimental work [24].

IV. RESULTS AND DISCUSSIONS

Figure 7 presents the numerical variations of collector outlet temperature for 3 volume flow rate with same conditions.

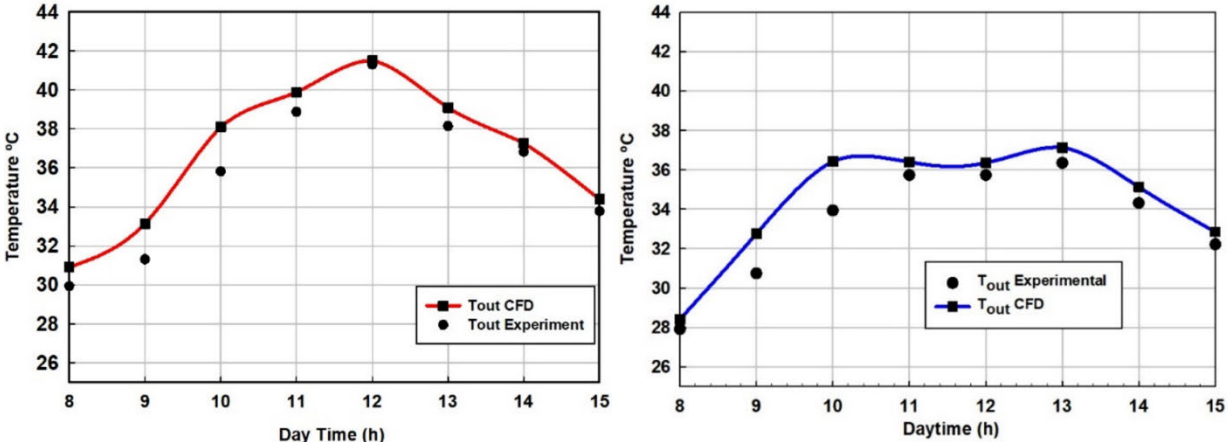

(a) DDW working fluid in first day of experimental.

(b)Alumina-water nanofluid in second day of experimental.

FIGURE 6. Model Validation with the experimental result in two different days of Hawash *et al.* [24].

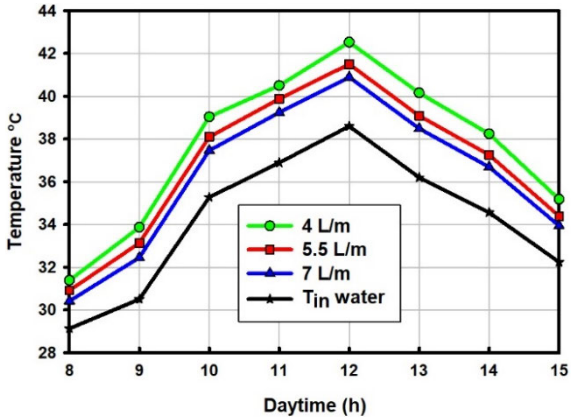

FIGURE 7. Variations of collector outlet temperature for three volume flow rates with same conditions.

The outlet temperature decreases with the increasing in volume flow rate. This figure is useful as FPSC used in the different application and it might be easy to control the outlet temperature. The FPSC was examined numerically for various volume flow rates of 4, 5.5, and 7 l/min for pure water.

Numerical simulations are conducted for DDW, Alumina and Copper oxide nanofluids with different volume fractions percentages. The temperature distributions of the working fluids, the pressure drop along the collectors and the thermal efficiency of the collector were estimated for each working fluid and each volume fraction percentage of the nanoparticle. Figure 8 shows the general behaviour of the working fluid temperature along with the pipe network of the absorber plate. As shown in the figure, the temperature of the fluid increases as it passes along the risers' pipes. Figure 9 shows the flow vectors inside the header and riser tubes at the inlet side of the collector.

Figure 10 shows the effect of the nanoparticle concentration on the pressure drop of the distilled water, Alumina oxide and copper oxide nanofluids in the collector for fluid flow rates of 5.5 L/s. The figure shows that; (i) increasing the nanoparticles' concentration in the fluids increases the pressure drop inside the collector. This can be attributed to the increase of the friction caused by increasing the fluid viscosity. (ii) The pressure drop decreases along with the daytime until it reaches its minimum at noon. It starts to increase with daytime, which can be attributed to the decrease of the working fluid's viscosity with the increase of the temperature. (iii) The pressure drop of the Copper oxide nanofluid inside FPSC is always higher than the pressure drop of the Aluminum oxide nanofluid and this can be attributed to the viscosities of the two fluids where for the same temperature and nanoparticle concentration, the viscosity of the Copper oxide nanofluid is higher than that of the Aluminum oxide nanofluid.

Figure 10 also illustrates that the pressure drop increases with a percentage in the range of 2-4% by increasing the nanoparticle concentration by 1%. Nevertheless, this percentage is noticeable; the effect of this value on the pump power can be considered negligible as compared to the gain of the heat transfer characteristics and the rise of the outlet temperature of the nanofluids. The pressure drop for the DDW is low as in the low concentration of alumina nanofluid. However, all concentration of copper oxide nanofluid results in high pressure drop compared with DDW as the density of copper oxide is high.

Figure 11 shows the impact of the alumina and copper oxide nanofluids volume fractions on collector efficiency. Figure 11-a shows that at low-temperature ranges, the collector's thermal efficiency in the case of using Alumina particle of low volume fraction 0.1% and 0.5% is slightly higher than those of the high volume fractions 1% and 2%. In another mean, the low concentrations of Alumina nanofluid are better than the high concentrations for the FPSC thermal efficiency. For example, Fig. 11-a illustrates that the maximum enhancement in the collector efficiency at the low-temperature difference is 2.32% at 0.1% volume fraction. However, at a high-temperature range, the collector's thermal

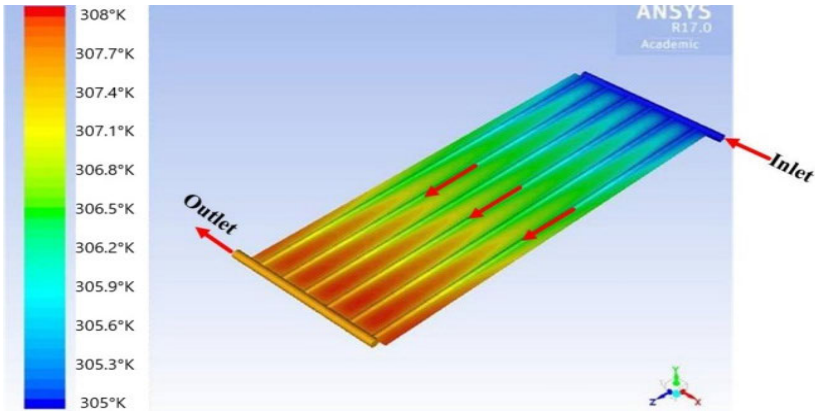

FIGURE 8. Temperature distribution via absorber plate, riser tubes, and collector headers.

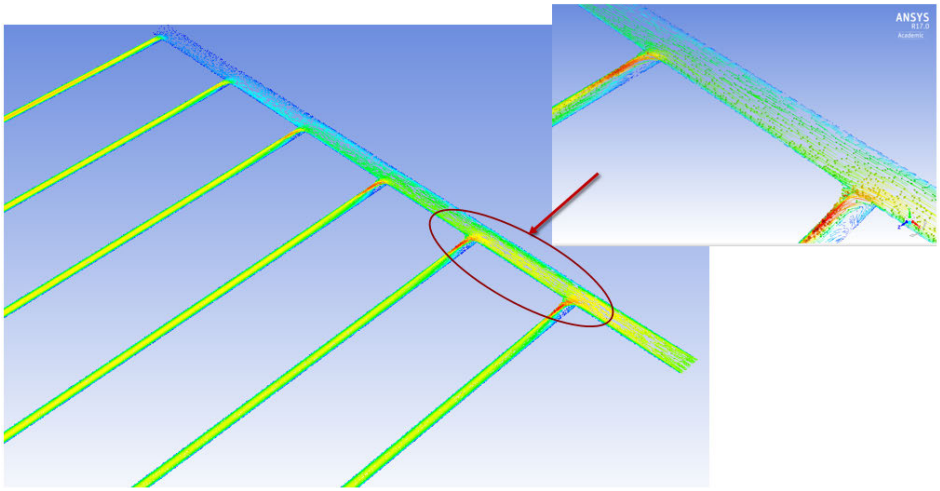

FIGURE 9. The flow vectors inside the header and riser tubes at the inlet side of the collector.

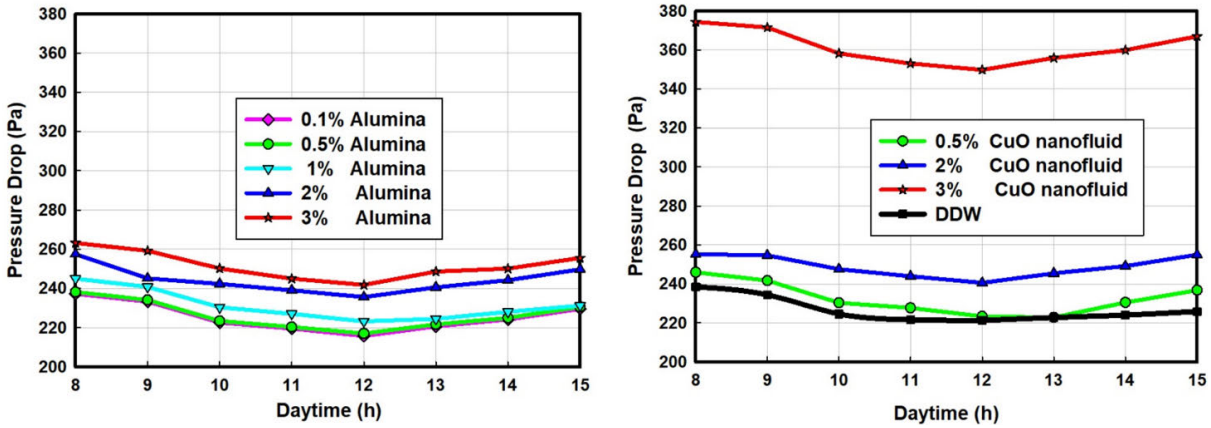

(a)Alumina nanofluid (b) Copper oxide nanofluid.

FIGURE 10. Effect of nanoparticles percentage on the working fluid's pressure drop at flow rate of 5.5 L/s.

efficiency in the case of using Alumina particle of high volume fractions 0.5%, 1% and 2% is higher than those of low volume fractions 0.1%. For example, the figure shows that the maximum enhancement in the collector efficiency at high-temperature differences range is about 2% at 0.5% volume fraction. Figure 11-b shows that at low-temperature ranges, the collector's thermal efficiency in case of using Copper oxide particle of volume fraction 0.5% and 1% is higher than those of volume fractions 0.1% and 2%. However, at a high-temperature range, the collector's thermal efficiency in the case of volume fractions 0.5% is higher than those of volume fractions 0.1 %, 1% and 2%.

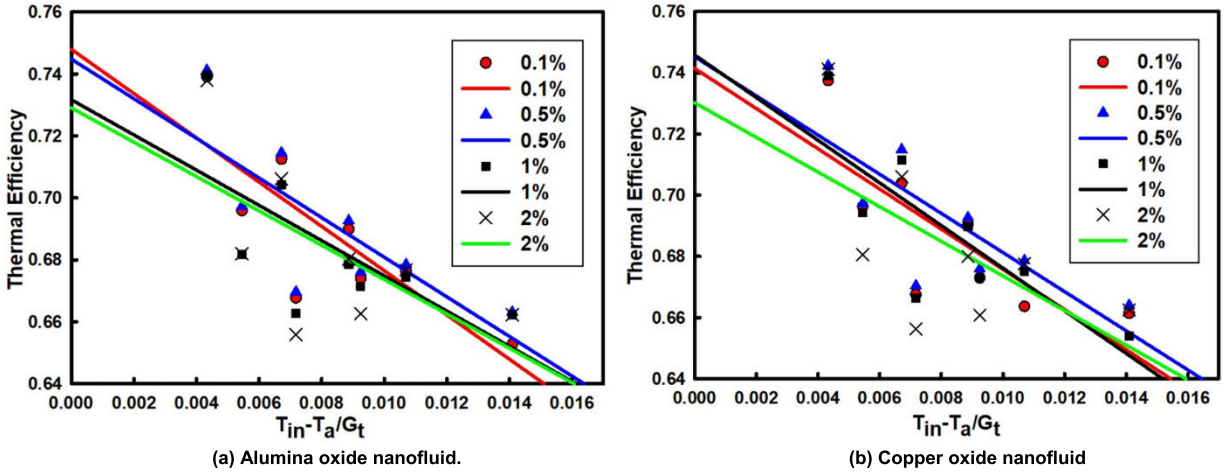

(a) Alumina oxide nanofluid. (b) Copper oxide nanofluid

FIGURE 11. Effect of nanoparticles volume fraction on the efficiency enhancement of the FPSC.

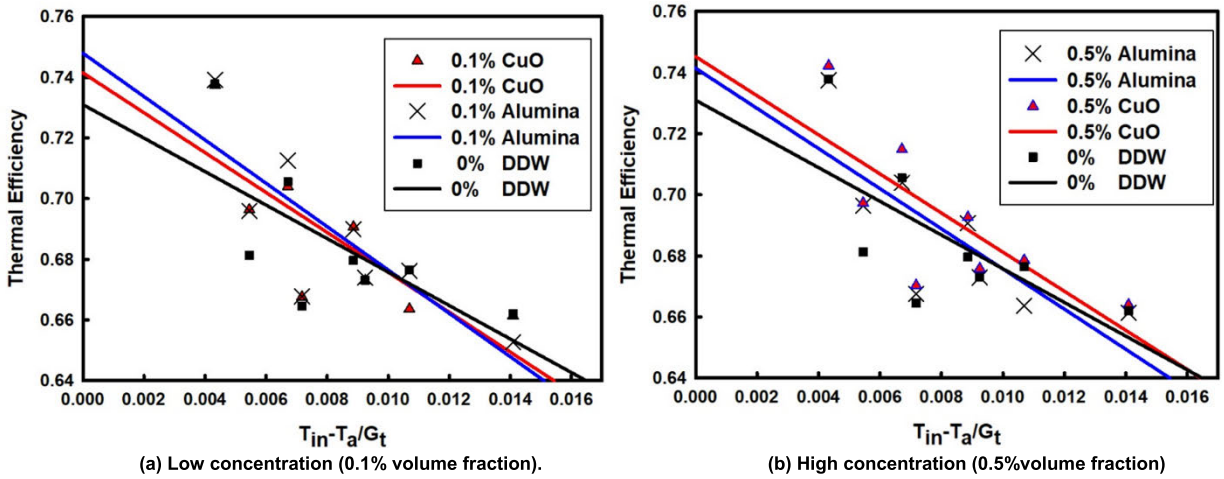

(a) Low concentration (0.1% volume fraction). (b) High concentration (0.5%volume fraction)

FIGURE 12. A comparison between the thermal efficiency of Copper oxide and Alumina nanofluids.

In general, Figure 11 shows that the average enhancement of the thermal efficiency at 0.5% volume fraction is significantly higher through the entire temperature range. It can be concluded that the efficiency of the FPSC increases with increasing the concentration of the Alumina or Copper oxide nanofluid until it reaches 0.5% and any further increase in the percentage of nanoparticle causes the decrease of the thermal efficiency.

This trend of the effect of the volume fraction of the nanoparticle on the collector efficiency can be attributed to (i) the increase of the thermal conductivity and the density of the fluid and the decrease of the viscosity with the increase of the concentration of the nanoparticles in the Alumina and Copper oxide nanofluid, (ii) at the low-temperature difference, the absorbed energy parameter is more controlling the thermal efficiency of the FPSC efficiency leading to more improvement in thermal efficiency at 0.1%-0.5% concentration, and (iii) the improvement at 0.5% volume fraction is significantly bigger all the time due to the increase of the thermal conductivity and thermal characteristics of the nanofluid with the increase of the concentration of the nanofluid until 0.5% and any further increase leads to the increase of the clustering and agglomeration which result in the decrease of the nanofluid thermal properties and the collector efficiency.

Figure 12 compares the two nanofluids' thermal efficiencies at the low nanoparticle concentrations (0.1%) and (0.5%), as these concentrations showed the desired enhancement. At 0.1%, the Alumina nanofluid performance is better than the Copper oxide nanofluid and at 0.5%, the Copper oxide nanofluid performance is more efficient than Alumina nanofluid. As an overall trend, it is seen that (i) the performances in the case of using the two nanofluids are higher than that of the DDW, and (ii) the overall performance in case of using copper oxide nanofluid is better than that of Alumina nanofluid.

The two parameters of the efficiency line of the FPSC are the intercept of the line with the vertical axes F_R $(\tau\alpha)$ and the slope of the line $(-F_R U_L)$. F_R $(\tau\alpha)$ represents the maximum

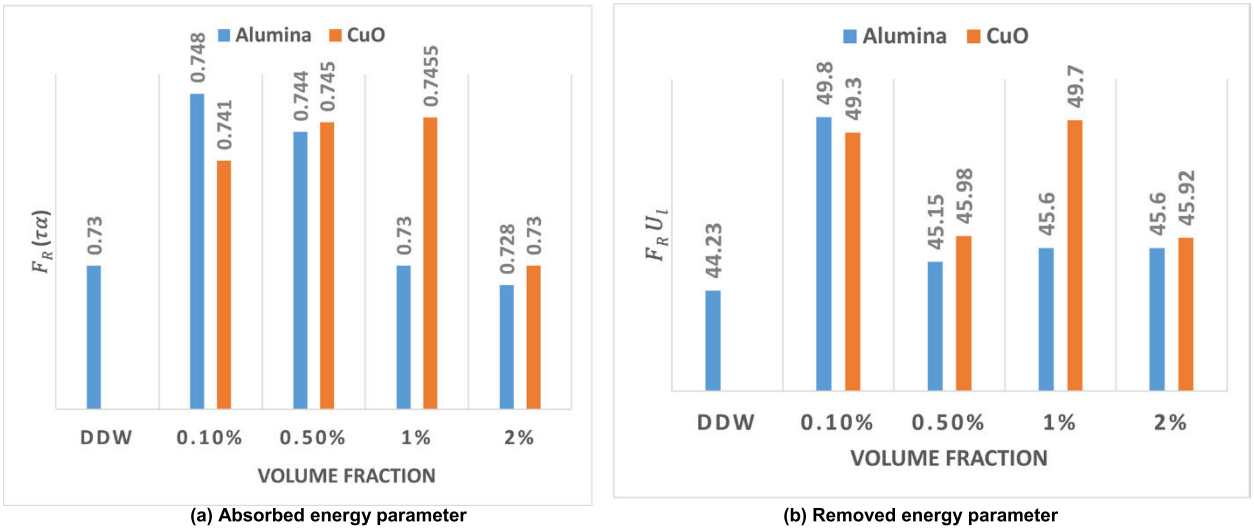

FIGURE 13. Efficiency performance parameter of FPSC for DDW and Alumina and Copper Oxide nanofluids of different percentages.

collector efficiency at fluid entering temperature to the collector equal to the ambient temperature. The collector efficiency becomes zero at the intersection of the efficiency line with the horizontal axis, which occurs at zero flow rate and is known as the stagnation point. The slope ($-F_R U_L$) of the line expresses the energy removal parameter from the collector. The efficiency lines parameters F_R $(\tau\alpha)$ and ($F_R U_L$) are presented in Fig. 13 for the different working fluids and nanoparticle fractions. The figure shows that (i) the value of F_R $(\tau\alpha)$ of Alumina nanofluid at 0.1% volume fraction concentration and for Copper oxide nanofluids at 0.5% and 1% volume fraction concentrations have the highest values compared with those of the nanofluid with other concentrations and DDW, (ii) the values of ($F_R U_L$) for Copper oxides nanofluid at 0.5% and 1% volume fractions are approximately the same, (iii) the value of ($F_R U_L$) for Alumina nanofluid at 0.1% volume fraction is slightly higher than those of the Copper oxide nanofluid at 0.5% and 1% concentrations, and (vi) the $F_R U_L$ of Copper oxide at 0.5% is much lower than those of alumina nanofluid of 0.1% concentrations and the Copper oxide of 1% concentrations. These trends of F_R $(\tau\alpha)$ and $F_R U_L$ for the different nanofluid and concentrations are the main reason for making the FPSC in case of using Copper oxide nanofluid with 0.5% volume fraction concentration has the best overall thermal efficiency.

V. CONCLUSION

A numerical study is developed to evaluate the thermal performance of the FPSC working with different fluids, including DDW and nanofluids of different nanoparticles material and nanoparticles percentage. CFD simulation was used for this purpose and validated by comparison with previous experimental results. The main goal of the study is to compare the performances of the different nanofluids and the different percentages of the nanoparticles. The results showed that (i) the presence of the nanoparticles in the working fluid slightly enhances the thermal performance of the collector, especially at low-temperature ranges, (ii) increasing the nanoparticles percentage in the nanofluids until 0.5% for the Alumina nanofluid and 1% for the Copper oxide nanofluid increases the thermal performance and any further increase in the nanoparticle percentage decreases the collector performance, (iii) in general the thermal performance of the Copper oxide nanofluid is better than that of the Alumina nanofluid, and (iv) increasing the nanoparticle percentage in the nanofluid increases the pressure drop by small percentages that do not affect the gain of the thermal performance of the collector.

ACKNOWLEDGMENT

It is a pleasure to acknowledge the Ministry of Higher Education (MoHE) of Egypt for providing a scholarship to conduct this study as well as the Egypt-Japan University of Science and Technology (E-JUST) for offering the facility, tools, and equipment needed to achieve this research work.

REFERENCES

[1] *ASHRAE*, Standard 1980 (RA 89) 1, 2003, p. 86244, vol. 6, no. Ra 89.
[2] R. Elghamry, H. Hassan, and A. A. Hawwash, "A parametric study on the impact of integrating solar cell panel at building envelope on its power, energy consumption, comfort conditions, and CO_2 emissions," *J. Cleaner Prod.*, vol. 249, Mar. 2020, Art. no. 119374.
[3] H. M. S. Hussein, H. H. El-Ghetany, and S. A. Nada, "Experimental investigation of novel indirect solar cooker with indoor PCM thermal storage and cooking unit," *Energy Convers. Manage.*, vol. 49, no. 8, pp. 2237–2246, Aug. 2008.
[4] Z. Said, M. A. Sabiha, R. Saidur, A. Hepbasli, N. A. Rahim, S. Mekhilef, and T. A. Ward, "Performance enhancement of a flat plate solar collector using titanium dioxide nanofluid and polyethylene glycol dispersant," *J. Cleaner Prod.*, vol. 92, pp. 343–353, Apr. 2015.
[5] J. A. Duffie and W. A. Beckman, *Solar Engineering of Thermal Processes*, 4th ed. Hoboken, NJ, USA: Wiley, 2013.
[6] J. A. E. Choi and U. S. Stephen, "Enhancing thermal conductivity of fluids with nanoparticles," in *Proc. ASME Int. Mech. Eng. Congr. Expo.*, 1995, pp. 12–17.

[7] M. Gupta, V. Singh, R. Kumar, and Z. Said, "A review on thermophysical properties of nanofluids and heat transfer applications," *Renew. Sustain. Energy Rev.*, vol. 74, pp. 638–670, Jul. 2017.

[8] Z. Said, M. H. Sajid, M. A. Alim, R. Saidur, and N. A. Rahim, "Experimental investigation of the thermophysical properties of AL_2O_3-nanofluid and its effect on a flat plate solar collector," *Int. Commun. Heat Mass Transf.*, vol. 48, pp. 99–107, Nov. 2013.

[9] L. S. Sundar, E. V. Ramana, Z. Said, V. Punnaiah, K. V. V. Chandra Mouli, and A. C. M. Sousa, "Properties, heat transfer, energy efficiency and environmental emissions analysis of flat plate solar collector using nanodiamond nanofluids," *Diamond Rel. Mater.*, vol. 110, Dec. 2020, Art. no. 108115.

[10] L. S. Sundar, Y. T. Sintie, Z. Said, M. K. Singh, V. Punnaiah, and A. C. M. Sousa, "Energy, efficiency, economic impact, and heat transfer aspects of solar flat plate collector with Al_2O_3 nanofluids and wire coil with core rod inserts," *Sustain. Energy Technol. Assessments*, vol. 40, Aug. 2020, Art. no. 100772.

[11] X. Zhang, H. Gu, and M. Fujii, "Effective thermal conductivity and thermal diffusivity of nanofluids containing spherical and cylindrical nanoparticles," *Experim. Thermal Fluid Sci.*, vol. 31, no. 6, pp. 593–599, May 2007.

[12] H. Xie, H. Lee, W. Youn, and M. Choi, "Nanofluids containing multiwalled carbon nanotubes and their enhanced thermal conductivities," *J. Appl. Phys.*, vol. 94, no. 8, pp. 4967–4971, 2003.

[13] V. Trisaksri and S. Wongwises, "Critical review of heat transfer characteristics of nanofluids," *Renew. Sustain. Energy Rev.*, vol. 11, no. 3, pp. 512–523, Apr. 2007.

[14] D. Wen, G. Lin, S. Vafaei, and K. Zhang, "Review of nanofluids for heat transfer applications," *Particuology*, vol. 7, no. 2, pp. 141–150, Apr. 2009.

[15] S. M. S. Murshed, K. C. Leong, and C. Yang, "Thermophysical and electrokinetic properties of nanofluids—A critical review," *Appl. Thermal Eng.*, vol. 28, nos. 17–18, pp. 2109–2125, Dec. 2008.

[16] P. Keblinski, J. A. Eastman, and D. G. Cahill, "Nanofluids for thermal transport," *Mater. Today*, vol. 8, no. 6, pp. 36–44, Jun. 2005.

[17] K. S. Hwang, S. P. Jang, and S. U. S. Choi, "Flow and convective heat transfer characteristics of water-based Al_2O_3 nanofluids in fully developed laminar flow regime," *Int. J. Heat Mass Transf.*, vol. 52, nos. 1–2, pp. 193–199, Jan. 2009.

[18] V. I. Terekhov, S. V. Kalinina, and V. V. Lemanov, "The mechanism of heat transfer in nanofluids: State of the art (review). Part 2. Convective heat transfer," *Thermophys. Aeromech.*, vol. 17, no. 2, pp. 157–171, Jun. 2010.

[19] S. E. B. Maïga C. T. Nguyen, N. Galanis, and G. Roy, "Heat transfer behaviours of nanofluids in a uniformly heated tube," *Superlattices Microstruct.*, vol. 35, nos. 3–6, pp. 543–557, Mar. 2004.

[20] W. Yu and H. Xie, "A review on nanofluids: Preparation, stability mechanisms, and applications," *J. Nanomater.*, vol. 2012, Sep. 2012, Art. no. 435873.

[21] T. Yousefi, F. Veysi, E. Shojaeizadeh, and S. Zinadini, "An experimental investigation on the effect of Al_2O_3–H_2O nanofluid on the efficiency of flat-plate solar collectors," *Renew. Energy*, vol. 39, no. 1, pp. 293–298, Mar. 2012.

[22] H. Tyagi, P. Phelan, and R. Prasher, "Predicted efficiency of a low-temperature nanofluid-based direct absorption solar collector," *J. Sol. Energy Eng.*, vol. 131, no. 4, Nov. 2009, Art. no. 041004.

[23] A. A. Hawwash and A. K. Abdel-Rahman, "Experimental study of alumina nanofluids effects on thermal performance efficiency of flat plate solar collectors," in *Proc. 5th Annu. Int. Conf. Sustain. Energy Environ. Sci. (SEES)*, Feb. 2016, pp. 102–110.

[24] A. A. Hawwash, A. K. Abdel Rahman, S. A. Nada, and S. Ookawara, "Numerical investigation and experimental verification of performance enhancement of flat plate solar collector using nanofluids," *Appl. Thermal Eng.*, vol. 130, pp. 363–374, Feb. 2018.

[25] L. Lu, Z.-H. Liu, and H.-S. Xiao, "Thermal performance of an open thermosyphon using nanofluids for high-temperature evacuated tubular solar collectors," *Sol. Energy*, vol. 85, no. 2, pp. 379–387, Feb. 2011.

[26] T. P. Otanicar and J. S. Golden, "Comparative environmental and economic analysis of conventional and nanofluid solar hot water technologies," *Environ. Sci. Technol.*, vol. 43, no. 15, pp. 6082–6087, Aug. 2009.

[27] R. A. Taylor, P. E. Phelan, T. P. Otanicar, C. A. Walker, M. Nguyen, S. Trimble, and R. Prasher, "Applicability of nanofluids in high flux solar collectors," *J. Renew. Sustain. Energy*, vol. 3, no. 2, Mar. 2011, Art. no. 023104.

[28] M. Faizal, R. Saidur, S. Mekhilef, and M. A. Alim, "Energy, economic and environmental analysis of metal oxides nanofluid for flat-plate solar collector," *Energy Convers. Manage.*, vol. 76, pp. 162–168, Dec. 2013.

[29] T. P. Otanicar, P. E. Phelan, R. S. Prasher, G. Rosengarten, and R. A. Taylor, "Nanofluid-based direct absorption solar collector," *J. Renew. Sustain. Energy*, vol. 2, no. 3, May 2010, Art. no. 033102.

[30] L. Yu and D. Liu, "Single-phase thermal transport of nanofluids in a minichannel leyuan," in *Proc. Int. Mech. Eng. Congr. Expo.*, 2009, pp. 1–9.

[31] G. Colangelo, E. Favale, A. de Risi, and D. Laforgia, "A new solution for reduced sedimentation flat panel solar thermal collector using nanofluids," *Appl. Energy*, vol. 111, pp. 80–93, Nov. 2013.

[32] A. García, R. H. Martin, and J. Pérez-García, "Experimental study of heat transfer enhancement in a flat-plate solar water collector with wire-coil inserts," *Appl. Therm. Eng.*, vol. 61, no. 2, pp. 461–469, 2013.

[33] G. Gallavotti and J. V. Lienhard, "Foundations of fluid dynamics," *Appl. Mech. Rev.*, vol. 55, no. 4, p. B75, 2002.

[34] K. G. T. Hollands, T. E. Unny, G. D. Raithby, and L. Konicek, "Free convective heat transfer across inclined air layers," *J. Heat Transf.*, vol. 98, no. 2, p. 189, 1976.

[35] A. D. Culf and J. H. C. Gash, "Longwave radiation from clear skies in niger: A comparison of observations with simple formulas," *J. Appl. Meteorol.*, vol. 32, no. 3, pp. 539–547, Mar. 1993.

[36] J. S. Jayakumar, S. M. Mahajani, J. C. Mandal, P. K. Vijayan, and R. Bhoi, "Experimental and CFD estimation of heat transfer in helically coiled heat exchangers," *Chem. Eng. Res. Des.*, vol. 86, no. 3, pp. 221–232, Mar. 2008.

[37] M. Saqib, I. Khan, and S. Shafie, "Application of fractional differential equations to heat transfer in hybrid nanofluid: Modeling and solution via integral transforms," *Adv. Difference Equ.*, vol. 2019, no. 1, pp. 763–769, Dec. 2019.

[38] E. F. El-gazar, W. K. Zahra, H. Hassan, and S. I. Rabia, "Fractional modeling for enhancing the thermal performance of conventional solar still using hybrid nanofluid: Energy and exergy analysis," *Desalination*, vol. 503, no. Nov. 2020, Art. no. 114847.

[39] K. P. Gertzos, S. E. Pnevmatikakis, and Y. G. Caouris, "Experimental and numerical study of heat transfer phenomena, inside a flat-plate integrated collector storage solar water heater (ICSSWH), with indirect heat withdrawal," *Energy Convers. Manage.*, vol. 49, no. 11, pp. 3104–3115, Nov. 2008.

[40] C. T. Nguyen, F. Desgranges, N. Galanis, G. Roy, T. Maré, S. Boucher, and H. Angue Mintsa, "Viscosity data for Al_2O_3–water nanofluid—Hysteresis: Is heat transfer enhancement using nanofluids reliable?" *Int. J. Thermal Sci.*, vol. 47, no. 2, pp. 103–111, Feb. 2008.

A. A. HAWWASH received the B.Sc. degree in power mechanical engineering from the Benha Faculty of Engineering, Benha University, Egypt, in 2011, and the M.Sc. degree in energy resources engineering from the Egypt-Japan University of Science and Technology (E-JUST), Alexandria, Egypt, in 2016, where he is currently pursuing the Ph.D. degree in energy resources engineering. Since September 2018, he was working as a Visiting Research Fellow with the Material Science Engineering Department, In Mori lab, Tokyo Institute of Technology, Tokyo, Japan. His research related to solar energy and thermal heat storage.

MAQUSOOD AHAMED received the Ph.D. degree from Jamia Hamdard (Hamdard University), India, and the Ph.D. degree from the University of Dayton, OH, USA, in 2010. He is working as an Associate Professor with the King Abdullah Institute for Nanotechnology, King Saud University, Riyadh Saudi Arabia. He has a strong background in the field of nanotechnology. He has published more than 110 research papers of international repute. He was awarded BEST RESEARCH QUALITY (Research Excellence) from King Saud University, in 2017. He was also listed in Highly Cited Researcher for 2017 and 2018 by Clarivate Analytics (Web of Science).

S. A. NADA received the B.Sc. degree in mechanical power engineering from Zagazig University, Zagazig, Egypt, in 1987, and the M.Sc. degree in power mechanical engineering from Cairo University, Cairo, Egypt, in 1992. He is currently a Professor with the Mechanical Engineering Department, Benha Faculty of Engineering, Benha University, Benha, Egypt. He is currently working as a Vice President of Education and Academic Affairs in Egypt-Japan University of Science and Technology, E-JUST, Alexandria, Egypt. He has a strong experience in the consultations works of design, construction supervisions and management of the electromechanical systems of different buildings applications including universities and educational buildings, hospitals, Pharma factories, commercial and residential buildings and health care facilities. He is the author of about 75 scientific research articles published in leading international journals until 2018.

ALI RADWAN received the B.S. and M.S. degrees in mechanical engineering from the Faculty of Engineering, Mansoura University, Mansoura, Egypt, and the Ph.D. degree from the Egypt-Japan University of Science and Technology (E-JUST), in 2018. He worked as a Lecturer with the Department of Mechanical Engineering, Faculty of Engineering, Mansoura University, in 2018. He was working as a Visiting Research Fellow with the Tokyo Institute of Technology, Tokyo, Japan. His research interested in photovoltaic cooling, renewable energy, and heat transfer

ALI K. ABDEL-RAHMAN received the B.S. and M.S. degrees in mechanical engineering from the Faculty of Engineering, Assiut University, in 1977 and 1984, respectively. He worked as a Lecturer with the Department of Mechanical Engineering, Faculty of Engineering, Assiut University, in 1992. He is currently a Professor with the Department of Mechanical Engineering, Faculty of Engineering, Assiut University, since 2014. In 2012, he was working as a chairperson with the Energy Resources Engineering Department, Egypt-Japan University of Science and Technology (E-JUST). His research related to subjects such as heat transfer, fluid mechanics, thermodynamics, seawater desalination, membrane clarification, CFD, and renewable energy.